J|A|C|S
ARTICLES
Published on Web 05/25/2004

Design, Synthesis, and Photophysical Studies of a Porphyrin-Fullerene Dyad with Parachute Topology; Charge Recombination in the Marcus Inverted Region

David I. Schuster,*,† Peng Cheng,† Peter D. Jarowski,† Dirk M. Guldi,*,‡ Chuping Luo,‡ Luis Echegoyen,§ Soomi Pyo,§ Alfred R. Holzwarth,|| Silvia E. Braslavsky,|| René M. Williams,|| and Gudrun Klihm||

Contribution from the Department of Chemistry, New York University, New York, New York 10003, and Radiation Laboratory, University of Notre Dame, Notre Dame, Indiana 46556, Department of Chemistry, Clemson University, Clemson, South Carolina 29634, and Max Planck Institute for Bioinorganic Chemistry (formerly Strahlenchemie), D 45413 Mülheim, Germany

Received September 23, 2003; E-mail: david.schuster@nyu.edu; guldi.1@nd.edu

Abstract: As part of a continuing investigation of the topological control of intramolecular electron transfer (ET) in donor−acceptor systems, a symmetrical parachute-shaped octaethylporphyrin-fullerene dyad has been synthesized. A symmetrical strap, attached to *ortho* positions of phenyl groups at opposing meso positions of the porphyrin, was linked to [60]-fullerene in the final step of the synthesis. The dyad structures were confirmed by ^{1}H, ^{13}C, and ^{3}He NMR, and MALDI-TOF mass spectra. The free-base and Zn-containing dyads were subjected to extensive spectroscopic, electrochemical and photophysical studies. UV−vis spectra of the dyads are superimposable on the sum of the spectra of appropriate model systems, indicating that there is no significant ground-state electronic interaction between the component chromophores. Molecular modeling studies reveal that the lowest energy conformation of the dyad is not the C_{2v} symmetrical structure, but rather one in which the porphyrin moves over to the side of the fullerene sphere, bringing the two π-systems into close proximity, which enhances van der Waals attractive forces. To account for the NMR data, it is proposed that the dyad is conformationally mobile at room temperature, with the porphyrin swinging back and forth from one side of the fullerene to the other. The extensive fluorescence quenching in both the free base and Zn dyads is associated with an extremely rapid photoinduced electron-transfer process, $k_{ET} \approx 10^{11}$ s^{-1}, generating porphyrin radical cations and C_{60} radical anions, detected by transient absorption spectroscopy. Back electron transfer (BET) is slower than charge separation by up to 2 orders of magnitude in these systems. The BET rate is slower in nonpolar than in polar solvents, indicating that BET occurs in the Marcus inverted region, where the rate decreases as the thermodynamic driving force for BET increases. Transient absorption and singlet molecular oxygen sensitization data show that fullerene triplets are formed only with the free base dyad in toluene, where triplet formation from the charge-separated state is competitive with decay to the ground state. The photophysical properties of the P−C_{60} dyads with parachute topology are very similar to those of structurally related rigid π-stacked P−C_{60} dyads, with the exception that there is no detectable charge-transfer absorption in the parachute systems, attributed to their conformational flexibility. It is concluded that charge separation in these hybrid systems occurs through space in unsymmetrical conformations, where the center-to-center distance between the component π-systems is minimized. Analysis of the BET data using Marcus theory gives reorganization energies for these systems between 0.6 and 0.8 eV and electronic coupling matrix elements between 4.8 and 5.6 cm^{-1}.

Introduction

Artificial photosynthesis has been the impetus behind much research since the earliest days of modern photochemistry.[1] The heart of photosynthesis is the absorption of sunlight and the subsequent conversion of that excitation energy into chemical potential energy by inducing charge separation that persists for a significant period of time. In bacterial systems, which are most thoroughly understood,[2,3] photoinduced electron transfer (PET) occurs in a photosynthetic reaction center, in which the relevant small organic molecules, namely four bacteriochlorophylls, two

† New York University.
‡ Radiation Laboratory.
§ Clemson University.
|| Max Planck Institute.

(1) Ciamician, G. *Science* **1912**, *36*, 385.

(2) *The Photosynthetic Reaction Center*; Deisenhofer, J., Norris, J. R., Eds.; Academic Press: New York, 1993.

(3) (a) Gust, D.; Moore, T. A.; Moore, A. L. *Acc. Chem. Res.* **2001**, *34*, 40. (b) Gust, D.; Moore, T. A. In *The Porphyrin Handbook*; Kadish, K., Smith, K. M., Guilard, R., Eds.; Academic Press: New York, 1999; pp 153−190. (c) Wasielewski, M. R. *Chem. Rev.* **1992**, *92*, 435. (d) Balzani, V.; Moggi, L.; F. Scandola, F. In *Supramolecular Photochemistry*; Balzani, V., Ed.; Dordrecht, 1987; pp 1−28. (e) Gust, D.; Moore, T. A.; Moore, A. L. *Acc. Chem. Res.* **1993**, *26*, 198. (f) Meyer, T. J. *Acc. Chem. Res.* **1989**, *22*, 163.

10.1021/ja038676s CCC: $27.50

bacteriopheophytins, two quinones, and one carotenoid polyene, are embedded in a protein environment, which serves to maximize the rate and efficiency of charge separation (CS) and minimize the possibilities of charge recombination (CR).[2,3] A multistep electron transfer sequence along an energy gradient generates a transmembrane CS state, with a quantum yield of nearly unity, which preserves a significant fraction of the energy of the initial excited state. Because the positive and negative charges are separated by the thickness of the lipid bilayer, rapid charge recombination, which would waste the stored energy as heat, is precluded.

The simplest photosynthetic model systems involve interaction in solution of a photochemically active pigment and an additional electron donor (D) or acceptor (A), in which either of the following reactions might occur

$$D^* + A \rightarrow D^+ + A^- \rightarrow D + A$$

$$D + A^* \rightarrow D^+ + A^- \rightarrow D + A$$

While much fascinating electron transfer (ET) chemistry has been uncovered by such studies, these simple systems suffer from several crucial problems. Since bimolecular reaction kinetics in solutions are limited by diffusion, rate constants are on the order of 10^{10} M^{-1} s^{-1} at best. The very short lifetimes of the lowest excited singlet states of typical pigments (typically <10 ns), and their generally poor solubility precludes efficient ET from taking place. As a result, efficient intermolecular PET usually involves a triplet rather than a singlet excited state of the donor or acceptor component. A further, and ultimately quite serious, problem is that donor−acceptor (DA) separation and orientation are not fixed in fluid solution.

An obvious approach to achieve efficient and rapid ET is to covalently link donor and acceptor moieties, and indeed many types of donor−spacer−acceptor compounds have been synthesized and studied.[5] Early examples imitated photosynthetic reaction centers by using porphyrins as the pigments and covalently linked quinones as electron acceptors.[6] Although such PQ dyads do a good job of mimicking the gross features of the photoinduced charge separation step of the photosynthetic reaction center, back ET is typically quite fast, resulting in very short-lived CS states.

Recently, there has been a great deal of interest in C_{60} as the ultimate electron acceptor in multistep intramolecular PET reactions. Several comprehensive reviews of the literature of donor-C_{60} dyads and larger hybrids (triads, tetrads, pentads, etc) incorporating a wide variety of electron donors and linkers have been published.[3a,7] Not surprisingly, the greatest attention has been given to model systems in which porphyrins (P) are the electron donors. At the time this study was initiated some years ago, the two dyads which had been studied most thoroughly were **1** and **2**, in their free base (M = H_2) and Zn-complexed (M = Zn) forms (see Figure 1). In both systems, the chromophores are linked by bicyclic bridges created via a Diels−Alder reaction. Many of the fundamental properties of P−C_{60} dyads were revealed in these seminal studies, which will be very briefly summarized here.[8,9]

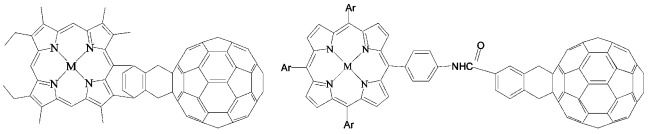

1 M = H_2 or Zn **2** M = H_2 or Zn Ar=3,5-di-*t*-butylphenyl

Figure 1. C_{60}-porphyrin dyads **1** and **2**.

Spectral data and molecular modeling on **1** and **1-Zn** indicate that there is some interaction between the two chromophores in their ground states.[8] The lifetimes of the porphyrin excited singlet states ($^1P^*$), from time-resolved fluorescence measurements, are ≤7 ps in toluene. The substantial quenching of $^1P^*$ is due to singlet−singlet energy transfer (EnT) from $^1P_{Zn}^*$ (2.1 eV) and $^1P^*$ (1.9 eV) to C_{60}. The lifetime of $P_{Zn}-{}^1C_{60}^*$ is ∼5 ps in toluene, while the singlet lifetime of a C_{60} model compound lacking the porphyrin is 1.2 ns. This secondary quenching is ascribed to ET to yield $P_{Zn}^{\bullet+}-C_{60}^{\bullet-}$ with $k \approx 2 \times 10^{11}$ s^{-1}. In toluene, $P-{}^1C_{60}^*$ does not undergo ET due to unfavorable thermodynamics. Instead, it decays by intersystem crossing (IC) to $P-{}^3C_{60}^*$. In the more polar solvent benzonitrile, $P-{}^1C_{60}^*$ undergoes ET to give $P^{\bullet+}-C_{60}^{\bullet-}$ with a rate constant of $\sim 2 \times 10^{11}$ s^{-1}.

At about the same time, Imahori and co-workers studied P−C_{60} dyads **2** and **2-Zn** and obtained quite similar results.[9] In general, it has been found that the dominant decay mode of photoexcited P−C_{60} dyads in nonpolar solvents (such as toluene and benzene) is energy transfer (EnT) to give an energetically lower-lying C_{60} excited singlet state, while in more polar solvents such as THF and benzonitrile, rapid PET occurs to yield the $P^{\bullet+}-C_{60}^{\bullet-}$ charge-separated state.[8−10]A critically important characteristic of P−C_{60} dyads is that the C_{60} moiety promotes photoinduced charge separation but retards the CR process. This observation has been ascribed to the small reorganization energy (λ) of C_{60} compared to λ for small electron acceptors such as quinones.[11,12] Since the charge in $C_{60}^{\bullet-}$ is spread over the whole C_{60} framework, the charge density is reduced at each carbon, which in turn reduces the solvent reorganization energy (λ_s). Since the rigid framework of C_{60} remains essentially unperterbed in $C_{60}^{\bullet-}$, the internal reorganiza-

(4) Diesenhofer, J.; Epp, O.; Miki, K.; Huber, R.; Michel, H. *J. Mol. Biol.* **1984**, *180*, 385. Yeates, T. O.; Korniya, H.; Chirino, A.; Rees, D. C.; Allen, J. P.; Feher, G. *Proc. Natl. Acad. Sci. U.S.A.* **1988**, *88*, 7993.
(5) Verhoeven, J. W.; Dirkxm L. P.; Deboer, T. J. *Tetrahedron Lett.* **1966**, 4399.
(6) For a review, see Gust, D.; Moore, T. A. *Top. Curr. Chem.* **1991**, *159*, 102. Kong, J.; Loach, P. A. In *Frontiers of Biological Energetics: From Electrons to Tissues*; Dutton, P. L., Leigh, J. S., Scarpa, H., Eds.; Academic Press: New York, 1978; Vol. 1, 73. Tabushi, I.; Koga, N.; Yanagita, M. *Tetrahedron Lett.* **1979**, 257.
(7) (a) Martin, N.; Sánchez, L.; Illescas, B.; Pérez, I. *Chem. Rev.* **1998**, *98*, 2527. Prato, M.; Maggini, M. *Acc. Chem. Res.* **1998**, *31*, 519. Guldi, D. M. *Chem. Commun.* **2000**, 321. (b) Bracher, P. J.; Schuster, D. I. In *Fullerenes: From Synthesis to Optoelectronic Properties*; Guldi, D. M., Martin, N., Ed.; Kluwer Academic Publishers: Dordrecht, 2002; pp 163−212.
(8) Liddell, P. A.; Sumida, J. P.; Macpherson, A. N.; Noss, L.; Seely, G. R.; Clark, K. N.; Moore, A. L.; Moore, T. A.; Gust, D. *Photochem. Photobiol.* **1994**, *60*, 537.
(9) Imahori, H.; Hagiwara, K.; Aoki, M.; Akiyama, T.; Taniguchi, S.; Okada, T.; Shirakawa, M.; Sakata, Y. *J. Am. Chem. Soc.* **1996**, *118*, 11 771.
(10) Liddell, P. A.; Kuciauskas, D.; Sumida, J. P.; Nash, B.; Nguyen, D.; Moore, A. L.; Moore, T. A.; Gust, D. *J. Am. Chem. Soc.* **1997**, *119*, 1400. Kuciauskas, D.; S. Lin, S.; Seely, G. R.; Moore, A. L.; Moore, T. A.; Gust, D.; Drovetskaya, T.; Reed, C. A.; Boyd, P. J. *J. Phys. Chem.* **1996**, *100*, 15926. Carbonera, D.; Di Valentin, M.; Corvaja, C.; Agostini, G.; Giacometti, G.; Liddell, P. A.; Kuciauskas, D.; Moore, A. L.; Moore, T. A.; Gust, D. *J. Am. Chem. Soc.* **1998**, *120*, 4398.
(11) Imahori, H.; Hagiwara, K.; Akiyama, T.; Aoki, M.; Taniguchi, S.; Okada, T.; Shirakawa, M.; Sakata, Y. *Chem. Phys. Lett.* **1996**, *263*, 545.
(12) For a review, see Guldi, D. M. In *Fullerenes: From Synthesis to Optoelectronic Properties*; Guldi, D. M., Martin, N., Eds.; Kluwer Academic Publishers: Dordrecht, 2002; pp 237−265.

tion energy (λ_i) is also small. Consequently, the CS rate is positioned near the peak of the Marcus parabolic curve relating k_{ET} to $-\Delta G°_{ET}$, that is, near the point where $-\Delta G°_{ET} = \lambda$. Since the thermodynamic driving force $-\Delta G°_{CR}$ in systems involving fullerenes is $>\lambda$, CR is pushed into the Marcus inverted region,[13] which enhances the lifetime of the CS state. This makes donor-C_{60} systems of particular interest as photosynthetic mimics and as components of photovoltaic devices.

Design of Novel C_{60}−Porphyrin Dyads

Both theory and experiment indicate that donor−acceptor distance and relative orientation play a crucial role in controlling the rate of PET, and consequently the efficiency of charge separation (CS) and the lifetime of the CS state. For Gust and Imahori's systems,[8,9] molecular modeling suggests that, when structurally possible, the dyads adopt the face-to-face conformation shown below, due to $\pi-\pi$ interaction between the two chromophores. This phenomenon is now known to be general, and is attributed to strong van der Waals attraction between porphyrin and C_{60} moieties, in the solid state as well as in solution.[14,15] Such conformations facilitate through-space dialogue between the donor and the acceptor, as demonstrated by efficient and rapid quenching of porphyrin fluorescence and generation of C_{60} excited states (by EnT) or $P_{Zn}^{\bullet+}-C_{60}^{\bullet-}$ CS states (by ET). To get more insight into the influence of molecular topology on PET, we became interested in the design and synthesis of P−C_{60} dyads in which the π-systems would be structurally forced into a face-to-face arrangement.

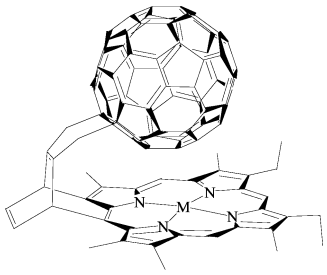

1

Two types of compounds have such structural topology, namely C_{60}−porphyrin cyclophanes **A** and parachute-shaped C_{60}−porphyrin dyads **B**. These are depicted schematically in Figure 2, where the circle represents a C_{60} moiety and the square represents a porphyrin. The design of the C_{60}-porphyrin cyclophane **A** is based on the fact that C_{60} can undergo controlled bis-addition using appropriate ligands (vide infra), whereas in the parachute-shaped dyad **B**, a strap controls the relative orientations of the C_{60} sphere and the porphyrin. Such compounds can be prepared using the versatile Bingel−Hirsch reaction, involving reaction of C_{60} with appropriate porphyrin-linked malonates in the presence of CBr_4 and DBU (1,8-diazabicyclo[5.4.0]undec-7-ene) as the base.[16,17]

Our efforts to prepare dyads of type **A** from strapped porphyrins synthesized using Baldwin's methodology[18] were ultimately unsuccessful, as mixtures of isomeric C_{60} bis-adducts were obtained which resisted separation by column chromatography on silica or HPLC. At precisely this time, Diederich and Hirsch independently reported the successful preparation of two dyads if this type, namely, **3** and **4**, shown below.[19,20]

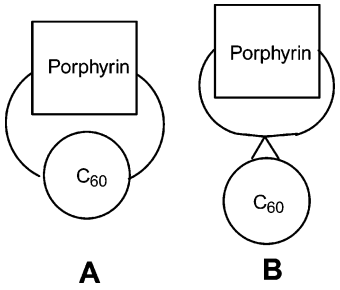

Figure 2. Face-to-face topology of porphyrin-C_{60} hybrids.

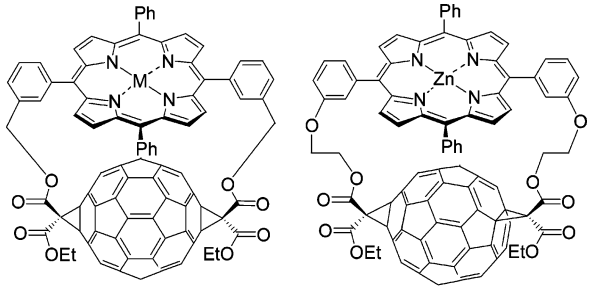

3 M = Zn or H_2 **4**

To synthesize these compounds, tethers with terminal malonate moieties were attached at meta positions of the 5,15-phenyl rings of a tetraphenylporphyrin (TPP) precursor. Diederich's dyad **3** was obtained as a *trans*-1 bis-adduct,[19] and Hirsch's dyad **4** as a *trans*-2 bis-adduct,[20] from two Bingel-Hirsch reactions. As a result of these reports, we abandoned our plans to prepare dyads of type **A**, and instead focused our attention on the synthesis and photophysics of a parachute-shaped C_{60}-porphyrin dyad of type **B**, namely compound **5**, shown below. Our efforts were successful, in part due to experience gained in attempts to prepare type **A** dyads.[21]

Results

Synthesis of the Parachute-Shaped C_{60}−Porphyrin Dyad 5. The central concept in the synthesis of dyad **5** was to anchor C_{60} to a malonate moiety inserted in a strapped porphyrin

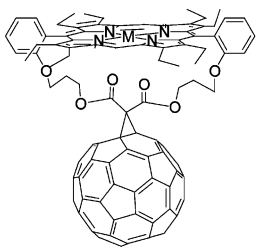

5 M = H_2 or Zn

derivative. The sequence of reactions for synthesis of such a porphyrin is shown in Scheme 1. Salicylaldehyde reacted with 3-bromopropanol in water to yield 2-(3-hydroxypropoxy)-benzaldehyde **6** in 73% yield. Coupling of **6** to malonyl dichloride gave bis-benzaldehyde **7** in 75% yield. Acid-catalyzed

(13) Marcus, R. A. *J. Chem. Phys.* **1956**, *24*, 966.
(14) Boyd, P. D. W.; Hodgson, M. C.; Rickard, C. E. F.; Oliver, A. G.; Chaker, L.; Brothers, P. J.; Bolskar, R. D.; Tham, F. S.; Reed, C. A. *J. Am. Chem. Soc.* **1999**, *121*, 10 487. Olmstead, M. M.; Costa, D. A.; Maitra, K.; Noll, B. C.; Phillips, S. L.; Van Calcar, P. M.; Balch, A. L. *J. Am. Chem. Soc.* **1999**, *121*, 7090.
(15) Schuster, D. I.; Jarowski, P. D.; Kirschner, A. N.; Wilson, S. R. *J. Mater. Chem.* **2002**, *12*, 2041.

Scheme 1. Scheme for Synthesis of Parachute Dyad **5**

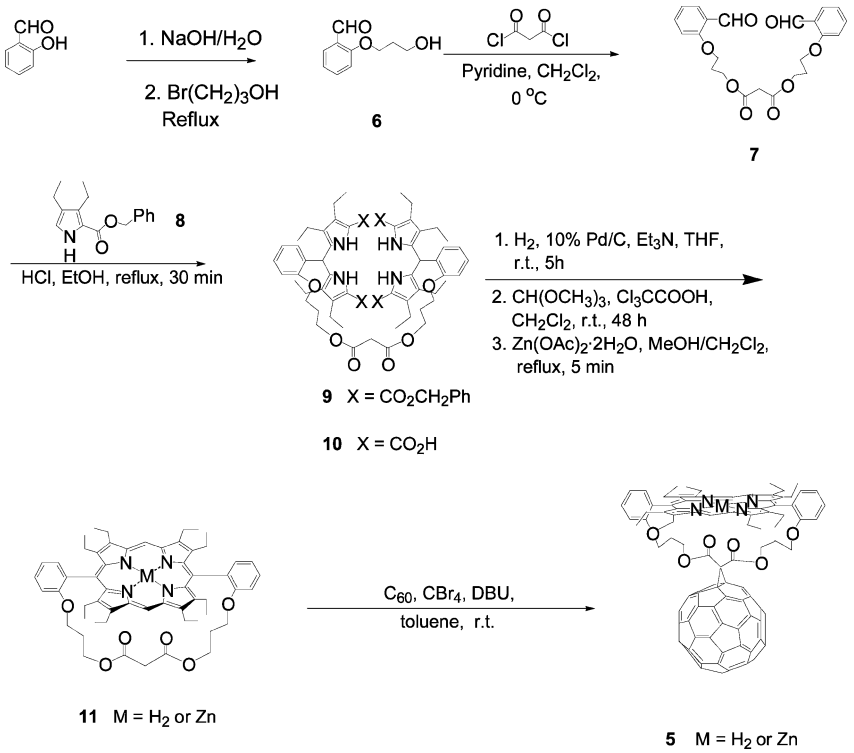

condensation of **7** with pyrrole **8**[22] afforded strapped-bis(dipyrromethane) **9** in 65% yield. After debenzylation by catalytic hydrogenolysis, the tetraacid **10** was reacted immediately with trimethyl orthoformate in CH_2Cl_2, using trichloroacetic acid as catalyst in the presence of zinc acetate, to give the desired strapped-porphyrin **11** containing the central malonate moiety in 15% yield. The crude reaction mixture of free-base porphyrin **11** and the corresponding zinc complex **11-Zn** was quantitatively converted to **11-Zn** by further treatment with $Zn(OAc)_2$ in a mixed solvent of CH_2Cl_2 and MeOH. In ^{1}H NMR spectra, the CH_2 protons of the malonate moiety of **11** were shifted upfield to δ 0.61 ppm compared to δ 3.30 in the precursor **9**, confirming that the strap resides over the aromatic porphyrin ring system.

Finally, the strapped porphyrin malonate **11** was attached to C_{60} via standard Bingel−Hirsch cyclopropanation, using CBr_4 and DBU.[17] Treatment of the reaction mixture with zinc acetate in refluxing CH_2Cl_2/MeOH gave the zinc porphyrin-C_{60} dyad **5-Zn**, isolated as a dark-purple crystalline solid in 25% yield using preparative TLC (silica gel, CH_2Cl_2/MeOH 25:1). The free-base dyad **5** was obtained by brief treatment of a CH_2Cl_2 solution of **5-Zn** with 5% aqueous HCl, followed by neutralization with aqueous $NaHCO_3$. Both **5** and **5-Zn** are crystalline solids with high melting points (>300 °C), and are quite soluble in relatively nonpolar organic solvents such as CH_2Cl_2, $CHCl_3$, and toluene, but not in polar solvents such as methanol and diethyl ether. After several washings with diethyl ether, the purity of the dyads according to TLC analysis was sufficient for structural characterization and photophysical studies.

Characterization of C_{60}−Porphyrin Dyad 5. The structure of the C_{60}-porphyrin dyad **5** was verified by spectral data, including ^{1}H NMR, ^{13}C NMR, ^{3}He NMR, UV−vis, and high-resolution mass spectra. As there are no protons on C_{60}, the ^{1}H NMR spectrum of **5** in $CDCl_3$ exhibits the expected features of the porphyrin and the strap with correct integration ratios. The spectrum of **5** is very similar to that of the strapped porphyrin **11** except for the disappearance of the two protons (δ 0.61) on the methylene carbon between the two carbonyl groups of the malonate. The ^{13}C NMR spectrum of **5** shows 9 resonances for the sp^3 carbon atoms, 24 of the 28 expected resonances in the region δ 97.0−160.0 for the sp^2 carbon atoms of the C_{60} moiety and the porphyrin, as well as a resonance (δ 162.0) for the malonate carbonyl groups (for details, see Supporting Information). This spectrum clearly demonstrates that dyad **5** has average C_{2v} symmetry on the NMR time scale (see Discussion below).

The existence of porphyrin and C_{60} moieties in dyad **5** was confirmed by its UV−vis spectrum, where strong absorption bands attributable to both moieties were observed. A high-resolution MALDI-TOF mass spectrum shows a molecular peak at m/z = 1621.5 (calcd. 1621.8), confirming that all the pieces are in place.

Recently, ^{3}He NMR, has been widely used in the characterization of fullerene compounds.[23] Saunders, Cross, and coworkers at Yale discovered that NMR-active ^{3}He can be

(16) Bingel, C. *Chem. Ber*. **1993**, *126*, 1957. Hirsch, A. *The Chemistry of the Fullerenes*; Georg Thieme Verlag: Stuttgart, 1994; Wilson, S. R., Schuster, D. I., Nuber, B., Meier, M. S., Maggini, M., Prato, M., Taylor, R. In *Fullerenes: Chemistry, Physics and Technology*; Kadish, K. M., Ruoff, R. M., Ed.; Wiley-Interscience: New York, 2000; pp 147−156.
(17) Camps, X.; Hirsch, A. *J. Chem. Soc., Perkin Trans. 1* **1997**, 1595.
(18) Baldwin, J. E.; Crossley, M. J.; Klose, T.; Orear, E. A.; Peters, M. K. *Tetrahedron* **1982**, *38*, 27. Baldwin, J. E.; Cameron, J. H.; Crossley, M. J.; Dagley, I. J.; Hall, S. R.; T. Klose, T. *J. Chem. Soc., Dalton* **1984**, 1739. Baldwin, J. E.; Perlmutter, P. *Top. Curr. Chem.* **1984**, *121*, 181.
(19) Bourgeois, J. P.; Diederich, F.; Echegoyen, L.; Nierengarten, J.-F. *Helv. Chim. Acta* **1998**, *81*, 1835.
(20) Dietel, E.; Hirsch, A.; Eichhorn, E.; Rieker, A.; Hackbarth S.; Roder, B. *Chem. Commun.* **1998**, 1981.
(21) Cheng, P.; Wilson, S. R.; Schuster, D. I. *Chem. Commun.* **1999**, 89.
(22) Barton, D. H. R.; Kervagoret, J.; Zard, S. Z. *Tetrahedron* **1990**, *46*, 7587.
(23) Saunders, M.; Jiménez-Vázquez, H. A.; Cross, R. J.; Mroczkowski, S.; Freedberg, D. I.; Anet, F. A. I. *Nature* **1994**, *367*, 256.

introduced into fullerene cages by heating them under high pressures of ^{3}He.[24] ^{3}He trapped inside the fullerene cages experiences a different magnetic environment from free ^{3}He. Thus, a characteristic signal at −6.3 ppm is observed for ^{3}He@C_{60} relative to gaseous ^{3}He used as the internal standard, set to 0 ppm.[23] In general, any product made from ^{3}He-labeled C_{60} yields a single sharp peak in its ^{3}He NMR spectrum, since altering the π-bonding structure of C_{60} affects the local magnetic field inside the cage and induces substantial ^{3}He chemical shifts. While typical [6,6] methanofullerenes such as Bingel adduct **12** (below) show a ^{3}He NMR resonance at δ −8.1,[24] dyad **5** prepared from ^{3}He@C_{60} shows a peak at δ −8.5 relative to ^{3}He gas (see Supporting Information). The upfield shift of 0.4 ppm is attributed to the shielding effect of the porphyrin ring current.

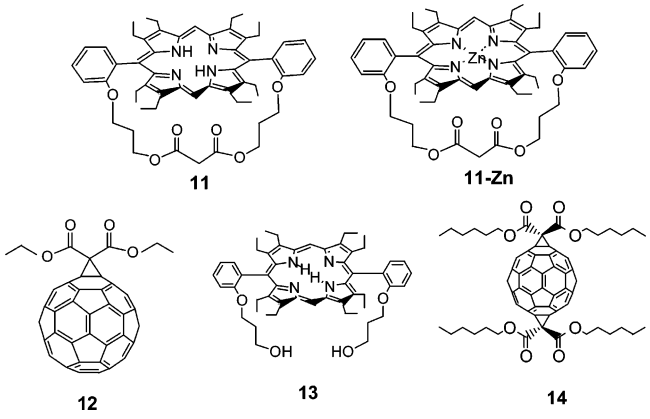

Confident that we had parachute-type porphyrin−C_{60} dyads **5** and **5-Zn** in hand, these materials were subjected to a series of steady state and time-resolved photophysical studies.

Electrochemical and Photophysical Properties of the C_{60}−Porphyrin Dyads 5 and 5-Zn

The physical and photophysical properties of the topologically novel dyads **5** and **5-Zn** were investigated by using various methods, including cyclic voltammetry, UV−vis absorption, fluorescence emission, time-resolved fluorescence emission, time-resolved transient absorption, and singlet oxygen measurements. For comparison data, all measurements were also performed on porphyrin model compounds **11** and **11-Zn** as well as C_{60} model compound **12**. Some of these data were reported in preliminary form in 1999.[26]

Electrochemical Studies. To estimate the energies of charge-separated states formed by PET, the electrode potentials for oxidation and reduction of the porphyrin and the functionalized C_{60} moiety, respectively, were determined by cyclic voltammetry (CV). For the potentiometric measurements, a BAS 100 W electrochemical analyzer (Bioanalytical System) was used (a 3 mm glassy carbon working electrode Ag/AgCl electrode as reference electrode, calibrated against the ferrocene/ferrocinium redox pair); the solvent used was dichloromethane containing 0.1 M tetra-*n*-butylammonium hexafluorophosphate as supporting electrolyte. These standard electrode potential data are summarized in Tables 1 and 2, together with comparison data for unstrapped porphyrin diols **13** and **13-Zn**.

Table 1. $E_{1/2}$ (V) Values for the Reduction Processes as an Average of the Cathodic and Anodic Peak Potentials[a]

compd	E_1	E_2	E_3	E_4	E_5
11	−2.01[b](88)[d]				
11-Zn	−2.18[b](94)				
5[c]	−1.09(71)	−1.45(76)	−1.90[b,e](103)	−2.00[b,e](128)	−2.25[b](66)
5-Zn[c]	−1.09(77)	−1.45(76)	−1.91(156)	−2.28(83)	−2.41[f]
13	−1.96[b](73)				
13-Zn	−2.21[b](105)				
12[c]	−1.06(80)	−1.42(78)	−1.88(136)	−2.28(88)	

[a] All values are relative to a Fc/Fc$^+$ internal reference. [b] irreversible processes. [c] At low temperature (−35 °C). [d] Values in parentheses are ΔE_{pp} (mV). [e] Overlapped peak. [f] Peak potential from OSWV.

Table 2. $E_{1/2}$ (V) Values for the Oxidation Processes as an Average of the Cathodic and Anodic Peak Potentials[a]

compd	E_1	E_2	HOMO–LUMO ($\Delta E_{1/2}$)[c]
11	0.27(80)[b]	0.56*(116)	2.28
11-Zn	0.08(53)	0.39*(54)	2.26
5	0.30(60)	0.56(56)	2.30
5-Zn	0.13(56)	0.39(56)	2.41/2.54[e]
14	0.30(58)	0.49[d](66)	2.26
14-Zn	0.06(68)	0.37[d](74)	2.28

[a] All values are relative to a Fc/Fc+ internal reference. [b] Values in parentheses are DEpp (mV). [c] For porphyrin subunits. [d] Irreversible processes. [e] From OSWV data.

The cyclic voltammogram of free-base C_{60}-porphyrin dyad **5** shows two reversible reductions with half-wave potentials ($E_{1/2}$) at −1.09 and −1.45 V (vs Fc/Fc$^+$) based on the fullerene core and two overlapping reductions ($E_{1/2}$ = −1.90 and −2.00 V), one corresponding to the fullerene and the other to the porphyrin, respectively (see Figure S1, Supporting Information). The reduction at −1.90 V is probably fullerene centered based on the results observed for model compounds **11** and **12**. The CV of zinc dyad **5-Zn** shows three reversible reductions at −1.09, −1.45 and −1.91 V (vs Fc/Fc$^+$) for the fullerene core.

Osteryoung Square Wave Voltammograms (OSWV) at low temperature (−35 °C) allowed better assignments (Figure S2). Compound **5** shows four reduction processes corresponding to the fullerene moiety (the first three and the fifth) and one reduction process (the fourth) corresponding to the porphyrin moiety. Due to significant cathodic shifts of the 4th and 5th reduction processes for **5-Zn**, it is not possible to state definitively whether these reductions are centered on the porphyrin moiety. Thus, while the OSWV observed for **5** is close to the sum of those observed for **11** and **12**, that for **5-Zn** is not the sum of those for **11-Zn** and **12**. The half-wave potentials for the reductions of compounds **5** and **5-Zn** corresponding to the fullerene moieties are more negative than those of the model compound **12** by ∼30 mV. The values of the reduction potentials for **5** are close to those reported for *trans*-1 C_{60} bisadduct **14** ($E^1_{1/2}$ = −1.09 V and $E^2_{1/2}$ = −1.47 V).[19]

The potentials for oxidation of **5**, **5-Zn**, **11**, and **11-Zn** are listed in Table 2. Generally, the zinc porphyrin compounds ($E_{1/2}$ = +0.08 V for **11-Zn** and $E_{1/2}$ = +0.13 V for **5-Zn**) are considerably easier to oxidize than the corresponding zinc-free porphyrin compounds ($E_{1/2}$ = +0.27 V for **11** and $E_{1/2}$ = +0.30 V for **5**) (see Figure S3). The first potential for oxidation of

(24) Saunders, M.; Jiménez-Vázquez, H. A.; Cross, R. J.; Mroczkowski, S.; Gross, M. I.; Giblin, D. E.; Poreda, R. J. *J. Am. Chem. Soc.* **1994**, *116*, 2193.
(25) Saunders, M.; Cross, R. J.; Jiménez-Vázquez, H. A.; Shimshi, R.; Khong, A. *Science* **1996**, *271*, 1693.
(26) Schuster, D. I.; Cheng, P.; Wilson, S. R.; Prokhorenko, V.; Katterle, M.; Holzwarth, A. R.; Braslavsky, S. E.; Klihm, G.; Williams, R. M.; Luo, C. P. *J. Am. Chem. Soc.* **1999**, *121*, 11 599.

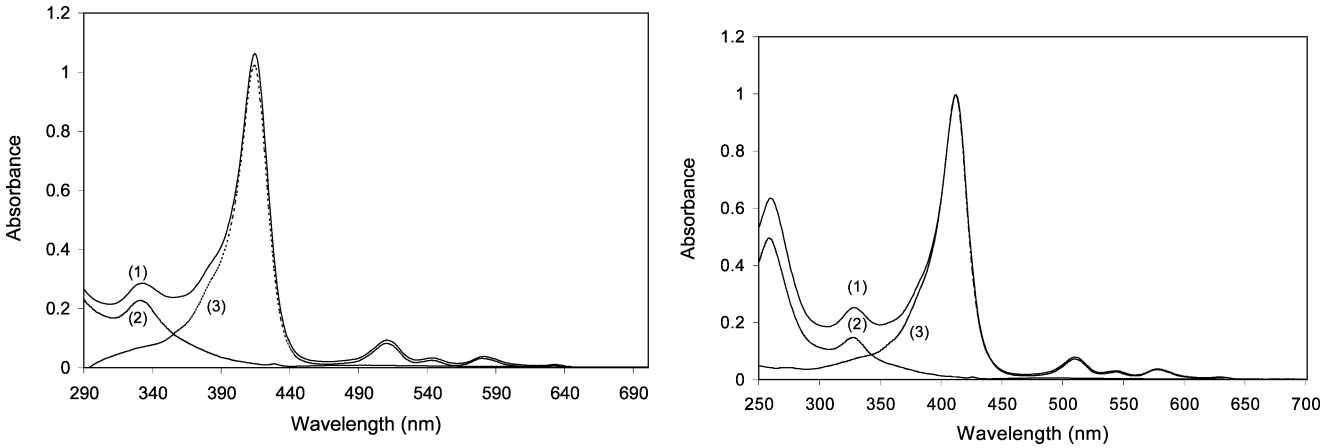

Figure 3. Absorption spectra of dyad **5** (1) and model compounds **12** (2) and **11** (3) in toluene solution (left) and CH_2Cl_2 solution (right); all concentrations were 5×10^{-6} M.

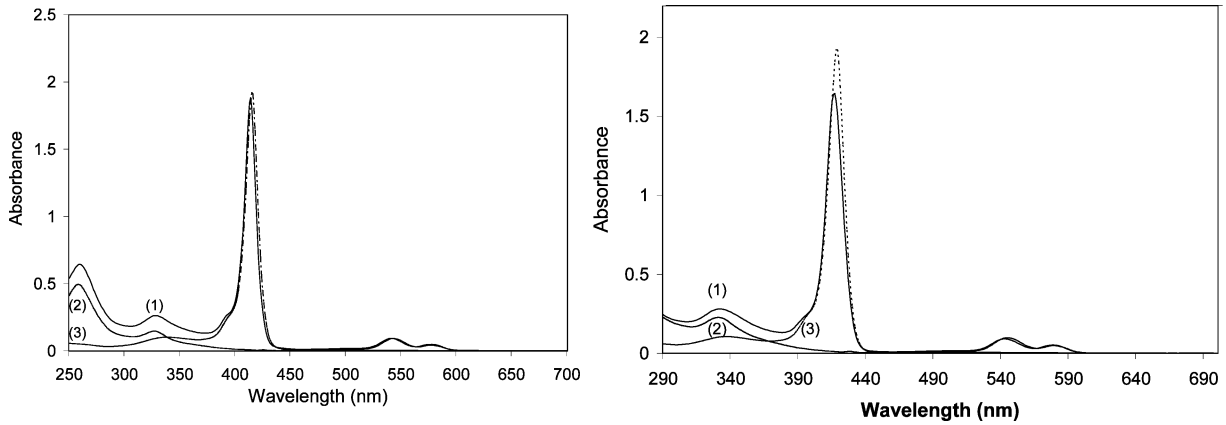

Figure 4. Absorption spectra of compounds **5** (1), **12** (2) and **11-Zn** (3) in toluene solution (left) and CH_2Cl_2 solution (right); all concentrations were 5×10^{-6} M.

11-Zn (+0.08 V vs. Fc/Fc^+) is unusually low compared with that of zinc *meso*-tetraphenylporphyrin (+0.29 V) and zinc octaethylporphyrin (+0.18 V).[27] This could arise as a consequence of an interaction between the carbonyl lone pairs and the porphyrin ring, which would increase the electron density in the latter. Structural effects sometimes result in easier oxidation, as seen for ring distortions of short-chain basket-handle porphyrins[28] and those induced by steric interaction from bromines at porphyrin β positions.[29] To assess the role of steric effects in the strapped porphyrin malonates **11** and **11-Zn**, the electrochemical data were compared with those for unstrapped porphyrin-diols **13** and **13-Zn**. No significant differences were observed, indicating that the molecular conformation in **11** has little effect on the oxidation processes. The two lowest potentials for oxidation of compounds **5** and **5-Zn** are ascribed to the porphyrin moiety. The half-wave potential for the first oxidation shifted to a more positive value than that of the model compounds by ~30 mV for **5** and ~50 mV for **5-Zn**.

Steady-State Absorption Spectra The absorption spectra of dyad **5** and **5-Zn** in toluene (nonpolar solvent) and CH_2Cl_2 (polar solvent) are essentially a linear combination of the absorption spectra of porphyrin reference compounds **11** and **11-Zn** and C_{60} reference compound **12** (Figures 3 and 4). In toluene, λ_{max} for the Soret band of the porphyrin in the free-base dyad **5** is at 414 nm, and the Q-bands appear at 510, 543, 581, and 633 nm (Figure 3, left), whereas the zinc dyad **5-Zn** features maxima at 417, 543, and 579 nm (Figure 4, left). In more polar solvents such as CH_2Cl_2, the absorption maxima of the dyads and the model porphyrins are blue shifted by 1−5 nm relative to those in toluene. These spectra suggest that there is no significant electronic interaction between the porphyrin and fullerene moieties in the ground state (however, see Discussion).

Steady-State Fluorescence Spectra. The fluorescence emission spectra of the dyads and model compounds were measured in both toluene and CH_2Cl_2. Figure 5 shows the emission spectra of dyad **5** and porphyrin reference **11** in toluene (top) and CH_2Cl_2 (bottom) solutions having equal absorbance at the excitation wavelength (580 nm). Porphyrin **11** shows fluorescence maxima at 635 and 698 nm with a fluorescence quantum yield Φ_F of 0.13, determined relative to that of 5,10,15,20-tetraphenylporphin (TPP), $\Phi_F = 0.11$.[30] C_{60} model compound **12** shows typically weak fluorescence at 715 and 798 nm. ($\Phi_F \approx 10^{-4}$).[31] The porphyrin emission of dyad **5** is efficiently quenched by the attached C_{60} in both toluene and CH_2Cl_2 by a factor of at

(27) Kadish, K. M.; Guo, N.; Caemelbecke, E. V.; Froiio, A.; Paolesse, R.; Monti, D.; Tagliatesta, P.; Boschi, T.; Prodi, L.; Bolletta, F.; Zaccheroni, N. *Inorg. Chem.* **1998**, *37*, 2358. Kadish, K. M.; Shiue, L. R. *Inorg. Chem.* **1982**, *21*, 3623. Fuhrhop, J.-H.; Kadish, K. M.; Davis, D. G. *J. Am. Chem. Soc.* **1973**, *95*, 5140.
(28) Kadish, K. M.; D'Souza, F.; Villard, A.; Autret, M.; Caemelbecke, E. V.; Bianco, P.; Antonini, A.; Tagliatesta, P. *Inorg. Chem.* **1994**, *33*, 5169. D'Souza, F.; Zandler, M. E.; Tagliatesta, P.; Ou, Z.; Shao, J.; Caemelbecke, E. V.; Kadish, K. M. *Inorg. Chem.* **1998**, *37*, 4567.
(29) Ravikanth, M.; Reddy, D.; Misra, A.; Chandrashekar, T. K. *J. Chem. Soc., Dalton Trans.* **1993**, 1137. Reddy, D.; Ravikanth, M.; Chandrashekar, T. K. *J. Chem. Soc., Dalton Trans.* **1993**, 3575.

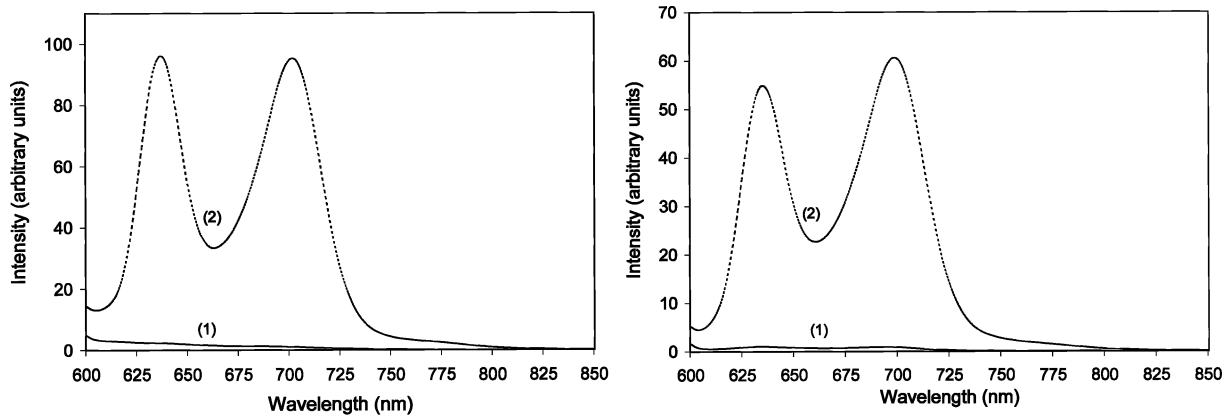

Figure 5. Steady-state fluorescence emission spectra of dyad **5** (1) and porphyrin model compound **11** (2) in toluene solution (left) and CH_2Cl_2 solution (right) with excitation at 580 nm; concentrations were 5×10^{-6} M.

Table 3. Fluorescence Lifetimes of Dyads

	fluorescence lifetimes τ_f (ns)[a,b]	
compd	benzene	THF
5	0.014 (0.904)	0.023 (0.819)
	0.057 (0.095)	0.08 (0.158)
5-Zn	0.009 (0.99)	0.013 (0.99)
11	13 (0.98)	11.3 (0.907)
11-Zn	1.81 (0.94)	1.8 (0.94)

[a] $\lambda_{exc} = 550$ nm, $\lambda_{obs} = 700$ nm for **5** and **11**, $\lambda_{obs} = 587$ nm for **5-Zn** and **11-Zn**. [b] Numbers in parentheses are relative amplitudes.

least 70, whereas no emission from the fullerene moiety was observed. Similarly, the fluorescence of **5-Zn** is strongly quenched by a factor of ~100 compared to that of **11-Zn** in both toluene and CH_2Cl_2 (not shown).

Time-Resolved Fluorescence Studies. Studies carried out at Mülheim by the single-photon counting method gave information concerning the dynamic behavior of the excited states of dyads **5** and **5-Zn**. These data are summarized in Table 3.

A solution of the free-base dyad **5** in benzene was excited at 550 nm, and emission decay profiles were collected at 700 nm. An analysis yielded two exponential decay components with lifetimes of 14 and 57 ps. The 14 ps component has a large amplitude (0.90) at the detection wavelength (700 nm), whereas porphyrin **11** emits strongly at this wavelength with a lifetime of 13 ns. Therefore, the dominant fluorescing species in the case of free base **5** is $^1P^*$, whose lifetime is shortened by a factor of ~1000 in benzene compared to **11**, which lacks the C_{60} moiety. This is consistent with the strong quenching of porphyrin fluorescence in dyad **5** detected in the steady-state experiments (see above). The 57 ps minor component to the fluorescence decay has not been definitively identified. It could be $P-^1C_{60}^*$, produced by singlet−singlet ET from $^1P^*-C_{60}$, which would be expected to decay by intramolecular ET to give the lower lying charge-separated (CS) state $P_{Zn}^{\bullet+}-C_{60}^{\bullet-}$.[7b,8−12]

Similar experiments were carried out with dyad **5-Zn** in benzene. Kinetic traces were collected at 587, 644 and 704 nm. The fluorescence decay was well-fitted with a single-exponential decay function with a lifetime of 9 ps, assigned to the excited ZnP moiety. As can be seen from these more quantitative data, the lifetime of $^1P_{Zn}^*$ in dyad **5-Zn** is shortened by a factor of ~200 compared with that for the model zinc porphyrin **11-Zn** (1.8 ns).

Time-resolved fluorescence studies carried out in tetrahydrofuran (THF) gave quite similar results. For dyad **5**, decay components with lifetimes of 23 and 80 ps were observed, with amplitudes of 0.82 and 0.16, respectively. The major component is the porphyrin S_1 state, whereas the latter is most likely the fullerene S_1 state. For **5-Zn**, a single fluorescing species was detected with a lifetime of 13 ps, attributed to $^1P_{Zn}^*$, more than 100-fold shorter than for model porphyrin **11-Zn**.

Transient Absorption Studies. The studies at Notre Dame were designed to detect nonemitting intermediates produced upon photoexcitation of **5** and **5-Zn**. Picosecond flash excitation at 532 nm of $\sim 10^{-5}$ M solutions of dyad **5-Zn** in toluene and benzonitrile afford the time-absorption profiles shown in Figure 6. Formation of porphyrin radical cations $P_{Zn}^{\bullet+}$ ($\lambda_{max} \approx 670$ nm)[8−12] on excitation of dyad **5-Zn** at 532 nm occurs within the time resolution of the apparatus (20−40 ps) in both nonpolar (toluene) and polar (THF, PhCN) solvents. Although $C_{60}^{\bullet-}$ ($\lambda_{max} \approx 1040$ nm)[8−12] was not directly detected due to experimental limitations at the time of these studies, it is assumed that this species is formed along with $P_{Zn}^{\bullet+}$. Similar studies with dyad **5** (data not shown) also reveal transient absorption for the porphyrin radical cation in the 500−760 nm region, again signaling formation of $P^{\bullet+}-C_{60}^{\bullet}$. Thus, extremely rapid electron transfer to give a charge-separated radical ion pair is the dominant decay pathway of $^1P^*$ in **5** and of $^1P_{Zn}^*$ in **5-Zn**, in both nonpolar and polar solvents. The CS states in turn decay by BET to regenerate ground-state starting materials, except for the free base dyad **5** in toluene where the C_{60} triplet state ($\lambda_{max} \approx 720$ nm)[31] is formed with a quantum yield of 0.22 (see below).

The CR dynamics were measured by the rate of decay of the porphyrin radical cation absorption at 650 nm. These data for **5** and **5-Zn** in six different solvents are collected in Table 4. There is clearly a strong dependence of the lifetimes of the CS ion-pair states of both **5** and **5-Zn** on solvent polarity. The trend is very clear: the lifetimes of the CS states decrease with increasing solvent polarity, i.e., the rates of BET increase as solvent polarity increases. Since stabilization of the CS state by solvation decreases the thermodynamic driving ΔG°_{CR} for charge recombination, BET for **5** and **5-Zn** must be occurring in the Marcus inverted region.[11−13] We will revisit this significant finding in the Discussion.

(30) Lee, W. A.; Graetzel, M.; Kalyansundaram, K. *Chem. Phys. Lett.* **1984**, *107*, 308.
(31) Guldi, D. M.; Prato, M. *Acc. Chem. Res.* **2000**, *33*, 695.

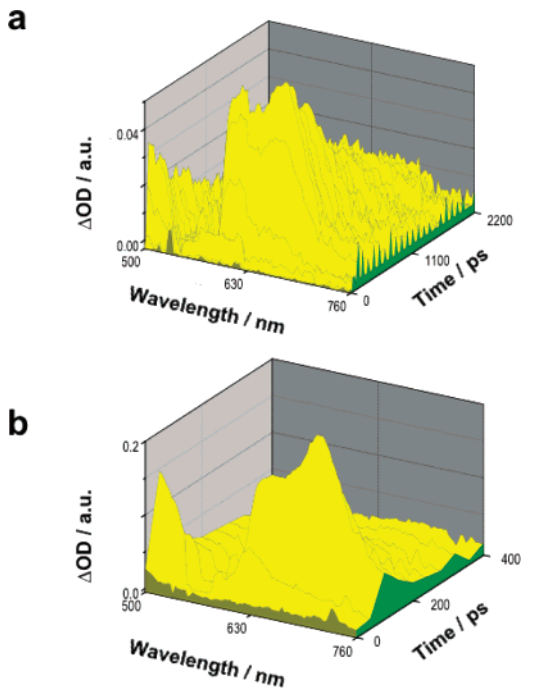

Figure 6. Time-resolved difference absorption spectra of ~10^{-5} M solutions of dyad **5-Zn** (a) in toluene at 100 ps intervals from from −100 to 2200 ps, and (b) in benzonitrile at 50 ps intervals of from −50 to 400 ps, after excitation at 532 nm.

Table 4. Lifetimes of the Radical Pair Charge Separated States of Dyads **5** and **5-Zn**[a]

solvent	relative static permittivity, ϵ_r[b]	**5** radical pair lifetime [ns]	**5-Zn** radical pair lifetime [ns]
toluene	2.38	3.5	1.015
tetrahydrofuran	7.58	0.314	0.099
dichloromethane	8.93	0.232	0.095
o-dichlorobenzene	9.93	0.201	0.095
benzonitrile	25.20	0.155	0.069
dimethylformamide	36.71	0.107	0.056

[a] Excitation at 532 nm; Detection at 650 nm. [b] Values from Murov, S. L.; Carmichael, I.; Hug, G. L. *Handbook of Photochemistry*, Second Edition; Marcel Dekker: New York, 1993; and *CRC Handbook of Chemistry and Physics*; CRC Press: Boca Raton, Florida.

Quantum Yields of Singlet Oxygen Production. It is well documented that C_{60} and its derivatives photosensitize the formation of singlet molecular oxygen, $O_2(^1\Delta_g)$, via triplet−triplet energy transfer, with an efficiency approaching 1.0.[32] Thus, studies of $O_2(^1\Delta_g)$ production are useful in probing the generation of triplet states upon excitation of porphyrin-C_{60} dyads. The quantum yields (Φ_Δ) for formation of $O_2(^1\Delta_g)$ from the dyads **5** and **5-Zn** and porphyrin reference compounds **11** and **11-Zn** were determined at Mülheim by measurements of the zero-time amplitudes of the $O_2(^1\Delta_g)$ luminescence decay at 1270 nm compared with 5,10,15,20-tetraphenylporphine (TPP) ($\Phi_\Delta = 0.67 \pm 0.14$ in toluene)[33] as the standard. All solutions were air-saturated and the excitation wavelength was 532 nm. As shown in Table 5, Φ_Δ for both **5** and **5-Zn** in CH_2Cl_2 is < 0.01; however, in toluene, Φ_Δ for **5** is 0.22, whereas that for **5-Zn** remains <0.01.

Table 5. Quantum Yields of Singlet Molecular Oxygen Formation from the Dyads **5** and **5-Zn** as Well as the Porphyrin References **11** and **11-Zn**

	singlet oxygen quantum yields Φ_Δ[a]	
compds	CH_2Cl_2[b]	toluene
5	<0.01	0.22 ± 0.02
5-Zn	<0.01	<0.01
11	0.96 ± 0.09	0.77 ± 0.08
11-Zn	0.80 ± 0.08	0.76 ± 0.08

[a] $\lambda_{exc} = 532$ nm, $\lambda_{obs} = 1270$ nm, TPP ($\Phi_\Delta = 0.67 \pm 0.14$) in toluene used as reference. [b] Corrected for differences in refractive index and $O_2(^1\Delta_g)$ radiative lifetime differences between the samples and the reference.

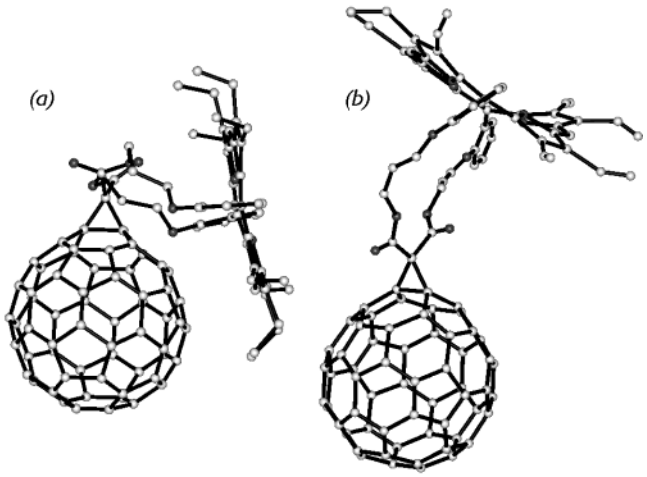

Figure 7. Bent and symmetric conformations of dyad **5**. The more stable structure is (a) on the left.

Discussion

Conformations of C_{60}−Porphyrin Dyad 5. The distance between the electron donor and acceptor in a D−A system is one of the key factors that controls the feasibility and kinetics of electron and energy transfer. This distance is regulated by the conformational properties of the system. Molecular modeling studies (InsightII 97.2, Discover 3) on the parachute-shaped C_{60}−porphyrin dyad **5**[15] reveal that in its lowest-energy conformation, Figure 7a, the porphyrin does not reside above C_{60} in a structure with C_{2v} symmetry, Figure 7b, as previously thought.[21,26] Rather, in its most stable conformation, the porphyrin ring system lies on the side of the C_{60} sphere, with a center-to-center distance r_{cc} (distance from the center of the porphyrin to the center of the fullerene) of ~7.8 Å compared with ~10 Å in conformation (b). This r_{cc} value corresponds to an edge-to-edge distance r_{ee} of ~4.2 Å, which is close to van der Waals contacts. The bent unsymmetrical conformation (a) is stabilized by attractive van der Waals forces between the porphyrin and C_{60} moieties, as previously proposed,[14] and as observed in many types of P−C_{60} dyads.[8,9,34,35] In the bent conformation (a), protons at C_{10} and C_{20} on the porphyrin ring occupy different chemical environments, and should therefore be differentiable by ^{1}H NMR. Only a single peak for these two protons is observed at δ 10.33 at room temperature. The ^{13}C NMR spectrum of **5** is also consistent with a C_{2v} symmetrical structure. Thus, either the computational predictions are

(32) Arbogast, J. W.; Darmanyan, A. P.; Foote, C. S.; Rubin, Y.; Diederich, F. N.; Alvarez, M. M.; Anz, S. J.; Whetten, R. L. *J. Phys. Chem.* **1991**, *95*, 11. Bensasson, R. V.; Bienvenue, E.; Dellinger, M.; Leach, S.; Seta, P. *J. Phys. Chem.* **1994**, *98*, 3492.
(33) Ogilby, P. R.; Foote, C. S. *J. Am. Chem. Soc.* **1982**, *104*, 2069.
(34) D. Kuciauskas, D.; Lin, S.; Seely, G. R.; Moore, A. L.; Moore, T. A.; Gust, D.; Drovetskaya, T.; Reed, C. A.; Boyd,. P. *J. Phys. Chem.* **1996**, *100*, 15926.
(35) Schuster, D. I. *Carbon* **2000**, *38*, 1607.

incorrect, or dyad **5** is conformationally mobile, with the porphyrin moiety swinging from one side of the fullerene sphere to the other, through the high energy C_{2v}-conformation (b). This could be confirmed from studies of the temperature dependence of its ^{1}H NMR spectrum. Since ET generally occurs most rapidly when the donor (porphyrin) and the acceptor (C_{60}) are closest together,[7−10] this process should be fastest in the bent conformation of **5**. To date, attempts to obtain X-ray quality crystals of **5** and **5-Zn** have been unsuccessful.

Energetics of Charge Separation and Charge Recombination in Dyads 5 and 5-Zn. To assess the feasibility of electron transfer between the photoexcited porphyrin and C_{60} in the dyads **5** and **5-Zn**, the free energy change associated with this process was estimated using eq 1.[36] $E°(D^{+\bullet}/D)$ is the standard electrode potential of the donor cation

$$\Delta G°_{ET}/\text{eV} = e[E°(D^{+\bullet}/D) - E°(A/A^{-\bullet})] - E_{00} - e^2/\epsilon_r r \quad (1)$$

radical resulting from the electron transfer, $E°(A/A^{-\bullet})$ is the standard electrode potential of the acceptor (both in V and relative to the same reference electrode), ϵ_r is the relative medium static permittivity of the solvent (i.e., the dielectric constant), e is the elementary charge, and r is the center-to-center distance between the ions.

Photoinduced electron transfer (PET) should occur most rapidly in the lowest energy bent conformation (a) of dyad **5**. This conformation was therefore utilized for the free energy calculation. The value of $\Delta G°_{ET}$ for electron transfer between the porphyrin S_1 state and C_{60} in the dyad **5** in CH_2Cl_2 was calculated as follows. The energy (E_{00}) of the porphyrin lowest excited singlet state of **5** in CH_2Cl_2 was estimated as 1.96 eV relative to the ground state, from the average of the longest wavelength absorption band and shortest wavelength emission band of the porphyrin moiety. The average center-to-center distance r between the porphyrin and the C_{60} moiety in the bent conformation of **5** was estimated to be 7.8 Å from molecular modeling.[15] Thus, in CH_2Cl_2, where $\epsilon_r = 9.08$, the Coulombic term $e^2/\epsilon_r r = 0.21$ eV. From cyclic voltammetry, $E°(D^+/D)$ for the porphyrin = 0.30 V and $E°$ $(A/A^{-\bullet})$ for the fullerene = −1.09 V, both vs Fc/Fc^+. From these data, a value of $\Delta G°_{ET} = -0.78$ eV was obtained for **5** in CH_2Cl_2. Accordingly, the charge-separated state $P^{\bullet+}-C_{60}^{\bullet-}$ lies 1.18 eV above the ground state in CH_2Cl_2. A similar calculation for the zinc dyad **5-Zn** gives $\Delta G°_{ET} = -1.11$ eV. Since the excitation energy $E^1{}_{00}$ for **5-Zn** is 2.12 eV, the CS state $P_{Zn}^{\bullet+}-C_{60}^{\bullet-}$ in CH_2Cl_2 lies 1.01 eV above the ground state.

For **5** and **5-Zn** in THF, which has a relative permittivity $\epsilon_r = 7.58$, similar to that of CH_2Cl_2 ($\epsilon_r = 9.08$), the values of $\Delta G°_{ET}$ from the porphyrin S_1 state to C_{60} were estimated to be −0.82 eV and −1.15 eV, respectively,

For calculation of $\Delta G°_{ET}$ for dyads **5** and **5-Zn** in a nonpolar solvent, such as toluene, the modified relationship in eq 2 was employed,[36,37] using the redox potentials measured in CH_2Cl_2

$$\Delta G°_{ET}/\text{eV} = e[E°(D^{+\bullet}/D) - E_{red}(A/A^{-\bullet})] - E_{00} - e^2/\epsilon_r r - (e^2/2)(1/r^+ + 1/r^-)(1/8.93 - 1/\epsilon_r) \quad (2)$$

where ϵ_r is the relative permittivity of toluene (2.38), and r^+ (4.8 Å) and r^- (5.6Å) are the ionic radii of porphyrin radical cation and C_{60} radical anion, respectively. Thus, using 0.30 V as the standard electrode potential for oxidation of the porphyrin, −1.09 V as the standard electrode potential for reduction of C_{60}, 1.95 eV as the excitation energy of the porphyrin, and 7.8 Å for the average center-to-center distance between the porphyrin and C_{60}, $\Delta G°_{ET}$ for dyad **5** in toluene was estimated to be −0.47 eV. Similarly, $\Delta G°_{ET} = -0.81$ eV was obtained for **5-Zn** in the same solvent, again assuming ET occurs in the bent conformation. Accordingly, the charge-separated states $P^{\bullet+}-C_{60}^{\bullet-}$ and $P_{Zn}^{\bullet+}-C_{60}^{\bullet-}$ reside at 1.48 and 1.31 eV above the ground states, respectively. These data are summarized in Table 6.

Table 6. Free Energy Changes and Energy Transfer Rate Constants in THF and Toluene[a]

compds	solvents	$E^1{}_{00}$[b] (eV)	$E^2{}_{00}$[b] (eV)	$\Delta G°_{ET}$ (eV)	ΔG_{CR} (eV)	k_{ET}[c] (10^{10} s^{-1})	k_{CR}[c] (10^9 s^{-1})
5	THF	1.96	1.80	−0.82	−1.15	4.3	3.2
	toluene	1.95	1.80	−0.47	0.09[c]	7.1[d]	0.29[e]
5-Zn	THF	2.12	1.80	−1.15	−0.97	7.7	10
	toluene	2.12	1.80	−0.81	−1.31	11[d]	0.98

[a] The energy calculations are based on the lowest energy-bent conformation (a) in Figure 7. [b] $E^1{}_{00}$ and $E^2{}_{00}$ are energies of the 0−0 transition between the S_1 and S_0 states for the porphyrin and C_{60}, respectively. [c] $k_{ET} = \tau_f^{-1} - \tau_{f\,(ref)}^{-1}$, and $k_{CR} = \tau_{cs}^{-1}$. [d] Derived from the fluorescence data in benzene (Table 3). [e] Charge recombination gives C_{60} triplet states as well as ground state dyad **5**.

Accordingly, PET is thermodynamically favored in nonpolar as well as polar solvents for both the free base dyad **5** and its zinc analogue **5-Zn**, which is rare if not unprecedented for porphyrin-C_{60} dyads. The energy of the fullerene S_1 state is 1.80 eV, based on the absorption and emission spectra of the fullerene reference compound **12**, while the energy of the T_1 state of C_{60} is 1.57 eV.[31] These energies were used to construct the diagrams in Figures 8 and 9, which show the energy levels estimated for all proposed intermediates and associated interconversion pathways.

Kinetics of Photoinduced Electron Transfer and Back Electron Transfer. The various pathways for decay of the singlet states of the dyad **5** and **5-Zn** can be discussed with reference to Figures 8 and 9. No convincing evidence was obtained for the intermediacy of discrete $P-{}^1C_{60}*$ states in the decay processes of $^1P*-C_{60}$, although this cannot be strictly excluded. If C_{60} singlet excited states were formed, then we would expect intersystem crossing to $^3C_{60}*$ to compete with ET, but C_{60} triplets were not detected by transient absorption in solvents other than toluene, and $O_2(^1\Delta_g)$ formation was observed only for dyad **5** in toluene. Under these conditions, the lifetime of $^1P*-C_{60}$ is given by eq 3,

$$1/\tau_f = k_{ET} + k_f \quad (3)$$

where τ_f is the lifetime of the porphyrin lowest singlet excited state.

The fluorescence decay rate constant k_f is estimated as 8.8×10^7 s^{-1} from the 11.3 ns lifetime of the lowest singlet excited state of the model porphyrin **11**. Thus, In THF, where $\tau_f = 23$ ps, $k_{ET} = 4.3 \times 10^{10}$ s^{-1} (Table 6), and the quantum yield of photoinduced electron transfer Φ_{et} is ∼1.0.

We conclude that intramolecular quenching by C_{60} of the porphyrin S_1 state in dyads **5** and **5-Zn** in CH_2Cl_2 as well as **5-Zn** in toluene occurs entirely by electron transfer (ET). If

(36) Rehm, D.; Weller, A. *Isr. J. Chem.* **1970**, *8*, 529.

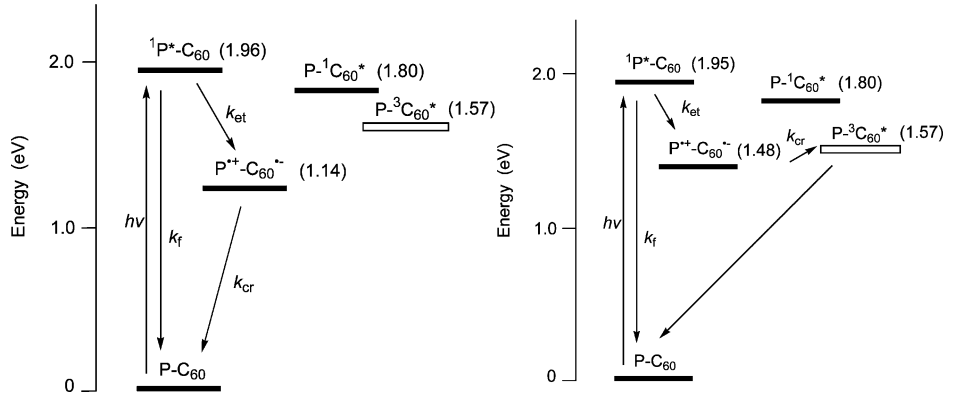

Figure 8. Energy states of dyad **5** in tetrahydrofuran (left) and toluene (right).

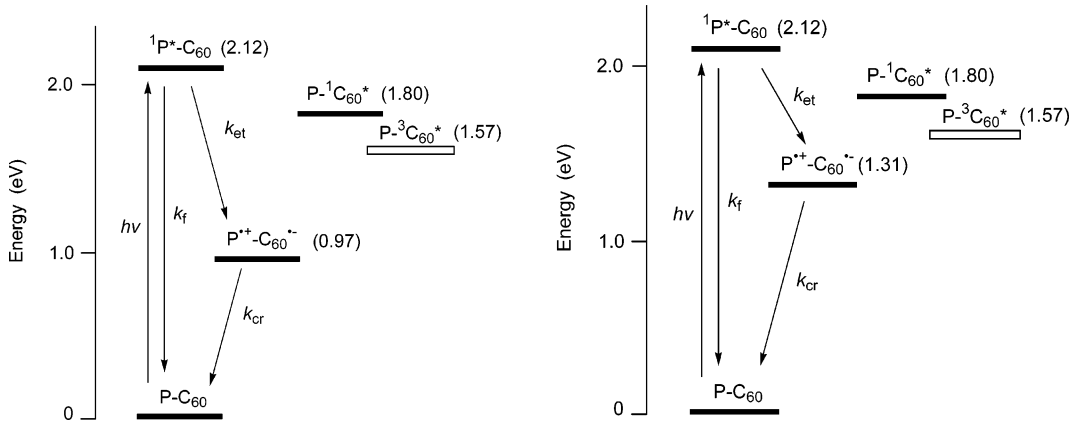

Figure 9. Energy states of dyad **5-Zn** in tetrahydrofuran (left) and toluene (right).

energy transfer (EnT) to give P−^{1}C$_{60}$* were involved, efficient intersystem crossing would occur to generate P−^{3}C$_{60}$*, which in turn would sensitize formation of $O_2(^1\Delta_g)$. In toluene, the production of $O_2(^1\Delta_g)$ ($\Phi_\Delta = 0.22 \pm 0.02$) upon excitation of **5** is attributed to the following sequence of events: (1) ET from the porphyrin to the C_{60} moiety to give the CS state; (2) back ET to give $^3C_{60}$*, in competition with regeneration of the dyad ground state; (3) EnT from $^3C_{60}$* to ground-state oxygen ($^3O_2$) to give $O_2(^1\Delta_g)$.[38] These results are consistent with the data obtained from time-resolved transient absorption studies, where C_{60} triplets were detected only upon excitation of **5** in toluene. We assume that k_{ET} for **5** in toluene is approximately the same as in benzene, i.e., 7.1×10^{10} s^{-1}. Similar kinetic data were obtained for **5-Zn**, as shown in Table 6, except that $O_2(^1\Delta_g)$ is not formed under any conditions investigated.

The magnitude of k_{ET} in both **5** and **5-Zn**, approaching 10^{11} s^{-1}, reflects the enforced proximity of the porphyrin to C_{60} and effective π, π-interactions. The fact that the charge separation rates are so large, and are very similar in benzene (toluene) and the much more polar THF, suggests that ET for **5** and **5-Zn** is occurring near the peak of the Marcus parabola.[12,13]

The CS states of **5** and **5-Zn** decay by charge recombination (CR) to their ground states, except for **5** in toluene where C_{60} triplet states are formed with a quantum efficiency of about 0.22. The lifetimes of the CS ion-pair states determined by the decay of porphyrin radical cation absorption at 650 nm were used to determine the rate constants k_{CR} shown in Table 6. The strong dependence of solvent polarity on the CS ion pair lifetimes of both **5** and **5-Zn** shown in Table 4 indicate strongly that BET (CR) occurs in the Marcus inverted region.[12,13,26]

Previously studied free-base C_{60}-porphyrin dyads and zinc-bound C_{60}-porphyrin dyads show two different patterns of photophysical behavior.[7−11,34,35] The dominant decay mode of photoexcited P−C_{60} dyads in nonpolar solvents (such as toluene or benzene) is energy transfer (EnT) to give a lower-lying fullerene singlet excited state, while in polar solvents such as benzonitrile, rapid photoinduced ET occurs to yield P$^{\bullet+}$−$C_{60}^{\bullet-}$ charge-separated states, occasionally in competition with somewhat slower singlet−singlet EnT to give fullerene singlet excited states. For ZnP−C_{60} dyads, PET usually dominates in nonpolar as well as polar solvents.[7b] Such behavior was shown by dyads **1** and **2**, as discussed earlier. In the case of **1**, it was concluded that through-space rather than through-bond electronic transfer dominates.[10]

It is useful to compare the results for dyads **5** with those for dyads **15**,[34] where competition between EnT and ET as a function of solvent polarity was also observed.

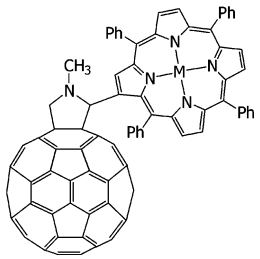

15a M = H_2
15b M = Zn

Perhaps the most significant finding in connection with the

present study is that values of τ_f in toluene for dyads **15**, 20−22 ps, are significantly longer than those of **5**, ∼14 ps, which is consistent with smaller values of r_{cc} for **5** (∼7 Å) than for **15** (9.9 Å). For **15** in toluene, it was concluded[34] that PET is negligible, as fluorescence quenching was attributed entirely to singlet−singlet EnT. In contrast, we conclude that for **5** ET dominates, even in toluene. The number of bonds separating the P and C_{60} moieties is much greater in **5** (10) than in **15** (2), but **5** is able to adopt a folded conformation (see Figure 7a), which is not accessible by **15**. Thus, through-space electronic interactions should dominate in the case of **5**, whereas only through-bond interactions are possible with **15**. The fact that rates of charge separation for **5** in THF (∼8 ps) and for **15** in PhCN (4−6 ps) are comparably fast suggests to us that topological differences between the two systems appear to have less influence on ET than on singlet−singlet EnT.

The observation of PET upon photoexcitation of zinc dyad **5-Zn** in both polar (THF, PhCN) and nonpolar (benzene, toluene) solvents fits the pattern observed for dyad **1b**[8,10] but not **15b**, where PET occurs only in polar solvents.[34] The magnitude of k_{ET} in both **5** and **5-Zn**, approaching 10^{11} s^{-1}, is similar to that in **1a** and **1b**, which suggests that strong π,π-interactions occur between porphyrin and C_{60} in both systems. The behavior of free-base dyad **5** is especially remarkable, in that ET prevails in the deactivation of ^{1}P* in both polar and nonpolar solvents, which is unprecedented. We attribute this to through-space interactions, since through-bond interactions (involving 10 bonds) are highly unlikely. Estimates of the energies of CS states from electrochemical data support the hypothesis that PET in **5** is exergonic in toluene as well as THF (see Table 6 and Figures 8 and 9). Because of the special topology of this dyad, intramolecular ET by electron exchange is much faster than singlet−singlet EnT by a Förster dipole−dipole mechanism. In toluene, where the CS state of **5** (1.48 eV) is destabilized so that it lies energetically close to the P−$^3C_{60}$* state (∼1.57 eV), decay to the latter with a spin flip[39] becomes energetically feasible. For **5** in toluene, there is no evidence that implicates P−$^1C_{60}$* or ^{3}P*−C_{60} states as precursors to P−$^3C_{60}$*, in contrast to the pathways proposed for dyads **1** and **15**.[8,10,34,38]

Our findings with compounds **5** and **5-Zn**, presented in preliminary form in 1999,[25] are completely in line with those reported more recently for the π−π-stacked ZnP−C_{60} dyad **4**.[40,41]In this C_2-symmetric dyad, the trans-2 linkage to the fullerene and the length of the tether enforces a face-to-face orientation of the two chromophores. As in dyad **5-Zn**, there are 10 bonds joining the porphyrin and fullerene moieties. The ZnTPP fluorescence in **4** is very strongly quenched in all solvents studied (toluene, THF, dichloromethane, dichloroethane, and benzonitrile). Fluorescence lifetimes were estimated to be ∼8.5 ps, corresponding to a quenching rate constant of 1.2×10^{11} s^{-1}, of the same order of magnitude as for **5-Zn** (13 ps). Transient absorption experiments on **4** demonstrate that ET prevails in all solvents, yielding the ZnTPP$^{\bullet+}$−$C_{60}^{\bullet-}$ CS state. The fact that ET rather than EnT dominates in the decay of the porphyrin singlet excited state of **4** was attributed to π-stacking of the two chromophores, which enhances electron exchange over a dipole−dipole energy transfer process, just as we propose above for **5**. The product of charge recombination of the CS state of **4** in all solvents except toluene is the singlet ground state. In toluene, a more complex decay process of the CS state of **4** (energy 1.54 eV) ensues, in which the first step is BET to give the ZnTPP triplet (energy 1.53 eV) followed by triplet−triplet EnT to give the fullerene triplet, Zn−TPP−$^3C_{60}$ (1.50 eV). New time-resolved EPR studies demonstrate that a similar pathway is followed by **5-Zn** in toluene.[38] In more polar solvents, where the CS state is energetically stabilized, charge recombination to give porphyrin and fullerene triplets is thermodynamically prohibitive. The fact that the lifetimes of the charge-separated state of **4** in THF (τ = 385 ps) and CH_2Cl_2 (τ = 122 ps) are significantly larger than those in the more polar solvents dichloroethane (τ = 61 ps) and benzonitrile (τ = 38 ps), shows that BET is occurring in the Marcus inverted region, where larger values of the thermodynamic driving force $-\Delta G°_{ET}$ lead to slower rates (k_{CR}).[12,13,41]

Thus, there is a very close similarity between the photophysical behavior of π-stacked dyads **5-Zn** and **4**, except for one very important difference: the pronounced red-shifts observed in the UV−vis spectra of **4** compared with appropriate model compounds, and the absence of such spectral shifts in the case of **5** and **5-Zn**. Indeed, we have observed substantial red shifts in absorption spectra of P−C_{60} dyads with flexible polyether linkers, where low energy conformations are readily accessible in which the two chromophores are in close proximity ($r_{cc} \approx$ 7−8 Å).[42] In the case of **4**, subtraction of the UV−vis absorption spectra of model compounds from the spectrum of **4** revealed a new broad band in the 700−800 nm region, assigned to a charge transfer (CT) transition between the porphyrin donor and the fullerene acceptors, confirming ground-state electronic interaction between the chromophores.[41] From the CT spectra the electronic coupling element V for **4** in toluene was estimated to be is 436 cm^{-1}. The failure to observe similar spectral features for **5-Zn**, which otherwise possesses strikingly similar photophysical properties, can be understood in terms of the differences in conformation of the two systems. The fullerene and porphyrin chromophores in **4** are rigidly held in a face-to-face topology, optimizing π-stacking and van der Waals interactions, whereas the flexibility of the linker in **5** permits the porphyrin ring system to move back and forth between conformations (see Figure 7a) in which van der Waals interactions are maximized, but are not permanently maintained. Thus, we attribute the absence of spectral shifts and CT absorption in **5-Zn**, despite rapid PET in both polar and nonpolar solvents, to the conformational flexibility in this system. Recent time-resolved EPR data at low temperatures also are consistent with PET from the bent conformation of **5-Zn**.[38] We hope to confirm

(37) Kavarnos, G. J. *Fundamentals of Photoinduced Electron Transfer*; VCH−Wiley: New York, 1993.
(38) Recent time-resolved electron paramagnetic resonance studies indicate that this process is more complicated: BET from the charge separated state of **5-Zn** in toluene first gives the lower lying porphyrin triplet state [^{3}ZnP*−C_{60}] which then undergoes triplet−triplet EnT to yield ZnP−$^3C_{60}$*: Galili, T.; Regev, A.; Levanon, H.; Schuster, D. I.; Guldi, D. M., submitted for publication.
(39) Kuciauskas, D.; Liddell, P. A.; Moore, A. L.; Moore, T. A.; Gust, D. *J. Am. Chem. Soc.* **1998**, *120*, 10880.
(40) Guldi, D. M.; Hirsch, A.; Scheloske, M.; Dietel, E.; Troisi, A.; Zerbetto, F.; Prato, M. *Chem. Eur. J.* **2003**. Guldi, D. M.; Luo, C.; Prato, M.; Dietel, E.; Hirsch, A. *Chem. Commun.* **2000**, 373.
(41) Guldi, D. M.; Hirsch, A.; Scheloske, M.; Dietel, E.; Troisi, A.; Zerbetto, F.; Prato, M. *Chemistry Eur. J.* **2003**, *9*, 4968.
(42) MacMahon, S.; Schuster, D. I., Unpublished results, quoted in MacMahon, S., Ph.D. Dissertation, New York University, 2003.

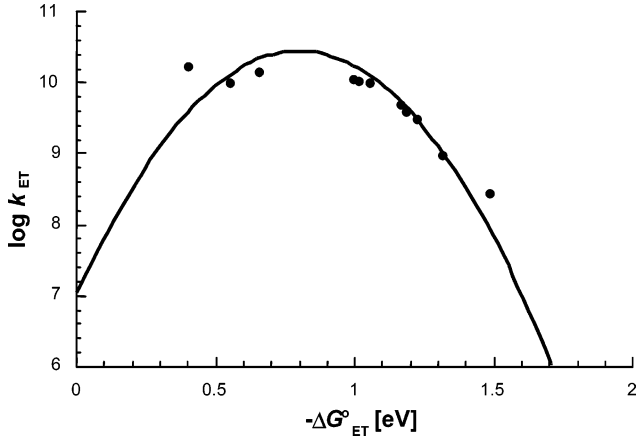

Figure 10. Plot of intramolecular electron-transfer rate constants in dyads **5** and **Zn-5** vs the thermodynamic driving force ($-\Delta G^{\circ}_{ET}$) The line represents the best fit ($\lambda = 0.80$ eV and V = 9.86 cm^{-1}).

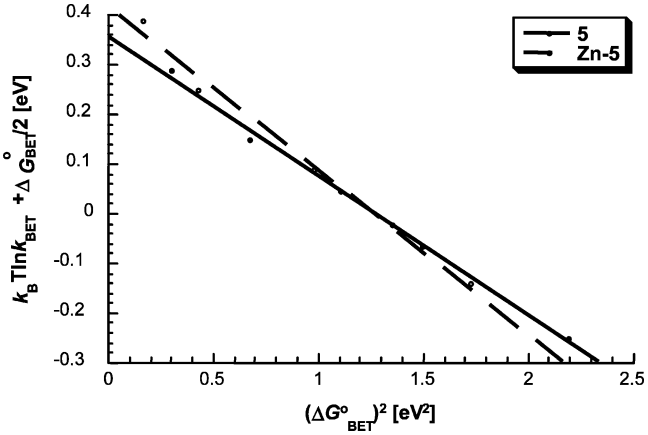

Figure 11. Plot of [k_BT ln k_{BET} + (ΔG°_{BET}/2)] vs (ΔG°_{BET})^2 for dyad **5** (solid line) and dyad **5-Zn** (dashed line).

this proposal by studies of the temperature dependence of spectral and photophysical properties of dyads topologically related to **5**.

Interpretation of Kinetics of Electron Transfer Processes in Dyads 5 and 5-Zn According to Marcus Theory. As concluded earlier, the thermodynamic driving force for PET (charge separation) in dyads **5** and **5-Zn** places this process near the peak of the Marcus parabola.[12,13] Back electron transfer (charge recombination), for which values of $-\Delta G^{\circ}_{CR}$ lie between 0.65 and 1.48 eV, places this process in the inverted region of the Marcus parabola, i.e., the highly exergonic region ($-\Delta G^{\circ} > \lambda$), where the ET rates decrease with increasing free energy changes.[11−13,41] A Marcus plot for dyads **5** and **5-Zn** was constructed from the ET rates, measured in several different solvents, and the values of the thermodynamic driving force ($-\Delta G^{\circ}_{ET}$), neglecting differences in the solvent polarity and solvent reorganization energy (see Figure 10). Values for $-\Delta G^{\circ}_{BET}$ were calculated for these dyads in *ortho*-dichlorobenzene, benzonitrile, and DMF following the procedure summarized in eq 1. From this plot, the total reorganization energies (λ) and electronic coupling matrix elements (V) for dyads **5** and **5-Zn** are estimated to be 0.8 ± 0.1 eV and 9.8 ± 1.0 cm^{-1}, respectively.

We then analyzed the driving force dependence on the rate constants, by applying eq 4, which can be transformed into the linear expression shown in eq 5, where k_B is the

$$k_{ET} = \left(\frac{4\pi^3}{h^2\lambda k_B T}\right)^{1/2} V^2 \exp\left[-\frac{(\Delta G^{\circ}_{ET} + \lambda)^2}{4\lambda k_B T}\right] \qquad (4)$$

$$k_B T \ln k_{ET} + \frac{\Delta G^{\circ}_{ET}}{2} = k_B T \ln\left[\left(\frac{4\pi^3}{h^2\lambda k_B T}\right)^{1/2} V^2\right] - \frac{\lambda}{4} - \frac{(\Delta G^{\circ}_{ET})^2}{4\lambda} \qquad (5)$$

Boltzmann constant.[13] Plots of [k_BT ln k_{BET} + (ΔG°_{ET}/2)] versus (ΔG°_{ET})^2 for BET give a linear correlation for both dyads, as shown in Figure 11. From this plot, the reorganization energy (λ) and electronic coupling (V) values obtained for dyad **5** are 0.71 eV and 4.8 cm^{-1}, respectively. A similar linear correlation for **5-Zn** afforded a slightly smaller λ-value, 0.61 eV, and V = 5.6 cm^{-1}.

Despite the assumptions, the two approaches are in good agreement. The λ values for **5** and **5-Zn** are slightly larger than those typically found for P−C_{60} dyads. For example, a reorganization energy of 0.59 eV was reported in a recent study involving several ZnP−C_{60} dyads with a series of spacers.[43] Larger reorganization energies are obtained when ground-state electronic interactions between the two chromophores prevail, as with π-stacked dyad **4**.[40,41] Thus, we propose that the reorganization energy can be used as an indicator of the degree of electronic interaction between the two chromophores.

The electronic coupling matrix elements V derived from the plot in Figure 11 are lower than that found for the π-stacked dyad **4**,[40,41] in line with the lack of CT features for **5** and **5-Zn**, in both the ground and excited states. Despite this, the BET rates in **4** and **5** are similar, which suggests electronic interactions exist in **5** and **5-Zn** which are not discernible spectroscopically.

Experimental Section

General Procedures. Unless specified, all reagents and solvents were purchased from commercial sources and were used as received. ^{3}He@C_{60} was obtained from Professor M. Saunders and Dr. A. Khong at the Chemistry Department of Yale University. Dry dichloromethane and toluene were freshly distilled over calcium hydride.

Moisture-sensitive liquids and solutions were transferred by syringes and introduced into reaction vessels through rubber septa. All the reactions were stirred magnetically unless noted otherwise. The progress of the reactions was monitored by thin-layer chromatography (TLC) whenever possible. TLC was performed using precoated glass plates (Silica gel 60, 0.25 mm thickness) containing a 254 nm fluorescent indicator. Spots were visualized using one of the following techniques: (a) 254 nm ultraviolet irradiation (UV); (b) insertion of the plates into a chamber containing a mixture of iodine crystals and silica gel. Flash chromatography was performed using ICN Silica 40−63 60 Å silica gel.

^{1}H and ^{13}C NMR spectra were obtained on either 200 or 300 MHz Varian Gemini NMR spectrometers. NMR samples were prepared in deuteriochloroform ($CDCl_3$). All chemical shifts are reported relative to an internal standard of tetramethylsilane. Steady-state absorption spectra were measured on a Genesys 5 UV−vis spectrophotometer. Fluorescence emission spectra were determined on a Perkin-Elmer LS 50 luminescence spectrophotometer.

(43) Imahori, H.; Yamada, H.; Guldi, D. M.; Endo, Y.; Shimomura, A.; Kundu, S.; Yamada, K.; Okada, T.; Sakata, Y.; Fukuzumi, S. *Angew. Chem., Int. Ed. Engl.* **2002**, *41*, 2344.

Benzyl 3,4-diethylpyrrole-2-carboxylate (8). To a solution of 3-acetoxy-4-nitrohexane (11.34 g, 60 mmol) and benzyl isocyanoacetate (11.37 g, 65 mmol) in 40 mL of THF was added DBU (19.44 mL, 130 mmol). The resulting mixture was stirred at room temperature for 16 h. The reaction mixture was then poured into water, and extracted with CH_2Cl_2. The combined organic layer was washed with H_2O and dried with Na_2SO_4 and then concentrated. Purification by column chromatography (silica gel, toluene) gave the desired product (10.6 g, 69% yield).

^{1}H NMR (200 MHz, $CDCl_3$): δ 1.20 (3H, t, J = 8.8 Hz), 1.24 (3H, t, J = 7.4 Hz), 2.44 (2H, q, J = 8.8 Hz), 2.76 (2H, q, J = 7.4 Hz), 5.30 (2H, s), 6.64 (1H, d), 7.3−7.4 (5H, m), 8.90 (1H, br). ^{13}C NMR (50 MHz, $CDCl_3$): δ 14.94, 15.58, 18.00, 18.22, 65.72, 118.34, 119.68, 127.02, 128.16, 133.09, 136.53, 161.33.

2-(3-Hydroxypropoxy)benzaldehyde (6). Salicylaldehyde (6.0 g, 49.1 mmol) was added dropwise to a solution of NaOH (2.0 g) in H_2O (80 mL), followed by dropwise addition of 3-bromo-1-propanol (5.6 g, 40.3 mmol). The mixture was heated on a steambath for 12 h and allowed to cool overnight. The solution was made strongly alikaline (pH $\approx$ 10) by the addition of NaOH and extracted with CH_2Cl_2 (4 × 50 mL). The combined organic phase was washed with brine (2 × 50 mL), dried over Na_2SO_4, filtered and concentrated to yield 2-(3-hydroxypropoxy)-benzaldehyde as an oil. Purification by column chromatography (silica gel, EtOAc:petroleum ether = 1:1) gave a clear oil (5.28 g, 73% yield).

^{1}H NMR (200 MHz, $CDCl_3$): δ 2.00 (2H, m), 3.66 (1H, s), 3.76 (2H, t), 4.10 (2H, t), 6.90 (2H, m), 7.42 (1H, m), 7.65 (1H, m). ^{13}C NMR (50 MHz, $CDCl_3$): δ 190.63, 161.39, 136.58, 129.83, 128.53, 125.04, 121.04, 113.02, 66.42, 59.82, 32.47.

Bis-3-(2-formylphenoxy)propyl Malonate (7). To a solution of 2-(3-hydroxypropoxy)benzaldehyde **6** (5.5 g, 30.6 mmol) in dry CH_2Cl_2 (100 mL) at 0 °C was added a solution of malonyl dichloride (2.2 g, 15.3 mmol) in 5 mL of CH_2Cl_2, followed by addition of triethylamine (5.1 g, 50 mmol). The resulting mixture was stirred at 0 °C for 1 h. The solution was then washed with water, dilute aqueous HCl, saturated aqueous sodium bicarbonate, and again with water. The organic phase was dried (Na_2SO_4) and concentrated in vacuo. Purification by column chromatography (silica gel, CH_2Cl_2:EtOAc = 100:7) gave the desired product **7** (5.0 g, 76%).

^{1}H NMR (200 MHz, $CDCl_3$): δ 2.20 (4H, m), 3.40 (2H, s), 4.12 (4H, t), 4.35 (4H, t), 7.00 (4H, m), 7.51 (2H, t), 7.80 (2H, d), 10.49 (2H, s). ^{13}C NMR (50 MHz, $CDCl_3$): δ 189.75, 136.35, 128.94, 121.41, 112.92, 65.32, 62.67, 41.96, 29.02.

Malonate-Strapped Dipyrromethane 9. A solution of dialdehyde **7** (4.35 g, 10.2 mmol) and pyrrole **8** (10.53 g, 41.0 mmol) in absolute ethanol (30 mL) was heated to reflux under nitrogen and concentrated hydrochloric acid (0.24 mL) was added. The reaction mixture was heated under reflux for 5 h, neutralized with concentrated NH_4OH, and concentrated in vacuo. The crude product was purified by column chromatography (silica gel, petroleum ether:EtOAc 3:1) to give the dipyrromethane **9** as a yellow foam (10.0 g, 69% yield).

^{1}H NMR (200 MHz, $CDCl_3$): δ 2.00 (2H, m), 3.66 (1H, s), 3.76 (2H, t), 4.10 (2H, t), 6.90 (2H, m), 7.42 (1H, m), 7.65 (1H, m). ^{13}C NMR (50 MHz, $CDCl_3$): δ 190.63, 161.39, 136.58, 129.83, 128.53, 125.04, 121.04, 113.02, 66.42, 59.82, 32.47.

Malonate-Strapped Octaethylporphyrin 11. A mixture of dipyrromethane **9** (2.84 g, 2.0 mmol), 10% Pd/C (0.75 g) and triethylamine (dry) (0.8 g) in dry THF (200 mL) was stirred under hydrogen until hydrogen uptake was complete. The solution was filtered through Celite and concentrated to dryness. The resultant foam of **10** was dissolved in dry CH_2Cl_2 (800 mL) and trimethyl orthoformate (4.60 mL, 41.9 mmol) and trichloroacetic acid (19.60 g, 120.0 mmol) were added. The reaction mixture was stirred in the dark, protected from moisture, for 5 h and zinc acetate (1.0 g) in dry methanol (15 mL) was added. The mixture was stirred for a further 48 h in the dark. The reaction mixture was washed with water, saturated sodium bicarbonate and water again. The organic phase was dried (Na_2SO_4) and concentrated to dryness in vacuo. The residue was dissolved in CH_2Cl_2 (20 mL) and heated at reflux. A solution of zinc acetate (1.0 g) in methanol (5 mL) was added and heating was continued for 5 min. The mixture was concentrated to dryness in vacuo and chromatographed on silica gel (CH_2Cl_2 with 1% Et_3N) to yield the desired zinc porphyrin **11** (138 mg, 12% yield).

^{1}H NMR (200 MHz, $CDCl_3$): δ −1.81 (2H, br), 0.62 (2H, s), 1.02 (4H, m), 1.36 (12H, t), 2.10 (12H, t), 2.45 (4H, t), 2.92 (4H, m), 3.20 (4H, m), 3.60 (4H, t), 4.21 (8H, q), 7.08 (2H, d), 7.57 (2H, t), 7.80 (2H, t), 8.57 (2H, d), 10.42 (2H, s). ^{13}C NMR (50 MHz, $CDCl_3$): δ 164.32, 159.64, 147.15, 145.65, 144.58, 143.71, 134.39, 132.90, 129.92, 119.74, 114.67, 112.34, 97.25, 65.41, 61.94, 38.95, 27.65, 21.37, 19.88, 18.73, 17.79.

C_{60}−Porphyrin Dyad 5. To a solution of zinc porphyrin **11** (166 mg) and C_{60} (620 mg, 5 eq) in toluene (350 mL) under nitrogen was added DBU (107 mg, 4 eq) and CBr_4 (70 mg, 1.2 eq). The resulting mixture was stirred overnight. Chromatography (silica gel, CH_2Cl_2 with 1% Et_3N) gave the desired dyad **5** (72 mg, 25% yield).

^{1}H NMR (200 MHz, $CDCl_3$): δ 1.11 (4H, m), 1.22 (12H, t), 1.97 (12H, t), 2.16 (4H, t), 2.72 (4H, m), 3.18 (4H, m), 3.80 (4H, t), 4.09 (8H, q), 7.13 (2H, d), 7.46 (2H, t), 7.80 (2H, t), 8.57 (2H, d), 10.33 (2H, s). ^{13}C NMR (75 MHz, $CDCl_3$): δ 161.53, 159.83, 145.44, 145.06, 144.98, 144.90, 144.53, 144.39, 144.29, 143.58, 142.85, 142.75, 142.67, 141.95, 141.61, 141.09, 140.62, 138.06, 134.03, 131.75, 130.45, 120.21, 113.46, 112.83, 97.27, 65.01, 63.37, 32.35, 27.89, 20.78, 19.91, 18.47, 17.48. ^{3}He NMR (500 MHz, 1-methylnaphthalene/$CDCl_3$): δ −8.5. UV−vis: λ_{max} (nm, CH_2Cl_2) (ϵ/dm^3 mol^{-1} cm^{-1}) 259 (115 600), 328 (44 400), 412 (138 000), 510 (10 000), 544 (6400), 577 (7600). MALDI-TOF (m/z): 1621.3 (M^+), calc. 1621.8 (M^+). Fluorescence (λ_{exc} = 580 nm) λ_{max} (CH_2Cl_2) 635, 698 nm.

Laser Flash Photolysis Experiments. Picosecond laser flash photolysis experiments were carried out with 532-nm laser pulses from a mode-locked, Q-switched Quantel YG-501 DP Nd:YAG laser system (18 ps pulse width, 2−3 mJ/pulse). Nanosecond Laser Flash Photolysis experiments were performed with laser pulses from a Quanta-Ray CDR Nd:YAG system (532 nm, 6 ns pulse width) in a front face excitation geometry.

Singlet Molecular Oxygen Emission Measurements. $O_2(^1\Delta_g)$ decays were measured upon excitation of air-saturated solutions of compounds **5**, **5-Zn**, **11**, and **11-Zn** with 8-ns laser pulses from the second harmonic of a Nd:YAG laser at 532 nm. The detector was a liquid N_2-cooled Ge-diode (Northcoast EO817FP) with a time resolution of 200 ns. The decay signals of 20 shots were averaged. Similar data were collected for the toluene solution of the reference (5,10,15,20-tetraphenylporphyrine, TPP). The absorbances of sample and reference solutions were $A_{532} = 0.1 \pm 0.002$. The ratio of the slopes of the zero-time extrapolated amplitude of the $O_2(^1\Delta_g)$ single-exponential decay vs the total laser energy per pulse (at low energy density where linearity is observed) for sample and reference solutions affords the ratio of quantum yields of $O_2(^1\Delta_g)$ production for the compound studied and the reference.[44] The $O_2(^1\Delta_g)$ lifetime in all CH_2Cl_2 solutions was $\tau_\Delta = 90 \pm 3$ μs and in toluene it was 30 ± 2 μs. Saturating the solutions with O_2 did not change the results.

Acknowledgment. The NYU group is grateful to the National Science Foundation for support of this study under grants CHE-009789 and CHE-9712735. The electrochemical studies at Clemson and Miami were also supported by the National Science Foundation. Studies at Notre Dame were supported by the U. S. Department of Energy. S.E.B., A.R.H, and their co-workers at Mülheim thank Prof. Kurt Schaffner for his support. This is contribution NDRL-4504 from the Radiation Laboratory.

(44) Wilson, S. R.; Yurchenko, M. E.; Schuster, D. I.; Yurchenko, E. N.; Sokolova, O.; Braslavsky, S. E.; Klihm, G. *J. Am. Chem. Soc.* **2002**, *124*, 1977.

Supporting Information Available: Cyclic voltammagrams and Osteryoung aquare wave voltammograms of compounds **5**, **5-Zn**, **11**, **11-Zn**, and **12** (Figures S1 to S3); 200 MHz ^{1}H NMR spectra of compounds **5**, **9**, and **11** (Figures S4 and S5); 50 MHz ^{13}C NMR spectrum of dyad **5** (Figure S6); MALDI-TOF mass spectrum of dyad **5** (Figure S7); ^{3}He NMR spectrum of dyad **5**. This material is available free of charge via the Internet at http://pubs.acs.org.

JA038676S